Energy Conversion and Management 93 (2015) 298–308

Contents lists available at ScienceDirect

Energy Conversion and Management

journal homepage: www.elsevier.com/locate/enconman

An experimental approach to improve the basin type solar still using an integrated natural circulation loop

Ahmed Rahmani [a,*], Abdelouahab Boutriaa [b], Amar Hadef [a]

[a] Department of Mechanical Engineering, University of Oum El Bouaghi, 04000, Algeria
[b] Department of Physics, University of Oum El Bouaghi, 04000, Algeria

ARTICLE INFO

Article history:
Received 10 September 2014
Accepted 10 January 2015
Available online 30 January 2015

Keywords:
Heat transfer
Mass transfer
Passive solar still
Natural circulation loop
Passive condenser

ABSTRACT

In this paper, a new experimental approach is proposed to enhance the performances of the conventional solar still using the natural circulation effect inside the still. The idea consists in generating air flow by a rectangular natural circulation loop appended to the rear side of the still. The proposed still was tested during summer period and the experimental data presented in this paper concerns four typical days. The convective heat transfer coefficient is evaluated and compared with Dunkle's model. The comparison shows that convective heat transfer is considerably improved by the air convection created inside the still. The natural circulation phenomenon in the still is studied and a good agreement between the experimental data and Vijajan's laminar correlation is found. Therefore, natural circulation phenomenon is found to have a good effect on the still performances where the still daily productivity is of 3.72 kg/m^2 and the maximum efficiency is of 45.15%.

1. Introduction

Solar desalination represents the most prominent and economical method especially when used in arid areas where sunshine is abundant and fresh water is scarce [1,2]. It represents an eco-friendly technology which can open up new water sources and contributes efficiently in the sustainable development of countries. Generally, the Conventional Solar Stills (CSS) are selected due to their simplicity and passive nature, no need for hard maintenance or skilled persons, which leads to little operation and maintenance costs. However, the CSS suffer from some drawbacks, which sometimes limit the use of this system for large-scale production [3]. Some of these drawbacks are, large solar collection area requirement, system vulnerability to weather-related damage, less market demand of technology and low interest of the manufacturers [4,5]. The main limitation is the low productivity compared with other desalination processes, where the daily yield from a single slope basin type solar still may vary from 0.5 to 2.5 kg/m^2 where its efficiency is usually about 5–40% [4,6]. Therefore, it is not cost-competitive with alternative methods.

The main factors affecting the still performances are meteorological conditions, design and operational parameters [7]. In fact, the meteorological parameters like solar intensity, wind velocity and ambient temperature cannot be controlled. Therefore, enhancing the still productivity can be achieved by a proper modifications in the still design and its operating parameters [8]. In the last 30 years, several experimental and theoretical investigations have been carried out to improve the CSS productivity by enhancing evaporation, condensation, heat storage and reducing thermal losses [9,10].

Reducing the water mass is always regarded as one of the key techniques to increase the still water temperature. Many articles focus on the investigation of this effect found that the highest outputs and efficiencies occur at lower depths [10,11]. Reflectors and concentrators are also used to increase water temperature at a faster rate by maximizing the amount of absorbed solar radiation [8,9,12]. Compared to the CSS, the daily productivity could be increased by 70–100% during winter days [13] and for the entire year it would average 48% with little enhancement for the summer days [14]. Sun-tracking systems are also used to increase the solar radiation amount. Abdallah et al. [15] introduced a sun tracking system to a fixed single-slope basin-type solar still. They found that the productivity increases by 22%.

Adding absorbing materials like dyes, wicks, glass balls, rubber, gravel, sand and saw dust are used as thermal storage materials in the basin liner. Rajvanshi [16] found that dye solution increases the single slope solar still productivity by 29%. The same improvement has been obtained by Badran [17] when using asphalt. Adding

* Corresponding author. Tel./fax: +213 32424192.
E-mail address: mag_phy@yahoo.fr (A. Rahmani).

http://dx.doi.org/10.1016/j.enconman.2015.01.026
0196-8904/

Nomenclature

A	flow cross section (m^2)
C	constant
Cp	heat capacity (J/kg °C)
D	flow hydraulic diameter (m)
f	friction factor, dimensionless
g	acceleration due to gravity (m/s^2)
Gr	Grashof number, dimensionless
Gr'	modified Grashof number, dimensionless
Gr_m	modified Grashof number
h_{cw}	convective heat transfer coefficient (W/m^2 °C)
h_{ew}	evaporative heat transfer coefficient (W/m^2 °C)
h_{rw}	radiative heat transfer coefficient (W/m^2 °C)
h_{fg}	latent heat of vaporization (J/kg)
HR	relative humidity (%)
I_o	solar intensity (W/m^2)
k	thermal conductivity (W/m °C)
m_d	hourly productivity (kg)
n	constant
NC	natural circulation
N_G	geometry number
Nu	Nusselt number
P	partial vapor pressure (N/m^2)
Pr	Prandtl number
Q	heat power (W)
T	temperature (°C)
W	mass flowrate (kg/s)

Greek symbol

β	thermal expansion coefficient (k^{-1})
ρ	density (kg/m^3)
μ	dynamic viscosity (Ns/m^2)
ε	emissivity, dimensionless
σ	Stefan–Boltzman constant (5.6697×10^{-8} W/m^2 k^4)
φ	relative humidity (%)

Indices

b	basin
C	col-leg
eff	effective
f	fluid
g	glass
H	hot-leg
i	inner
o	outer
r	relative, reference
s	sink
t	total
w	water

sponges in the basin liner, increases water evaporation due to capillary forces and the water absorption capacity. Velmurugan et al. [18] and Abu-Hijleh and Rababa [19] conducted experiments on a CSS when sponges were used. They found that the productivity was increased in the range of 15.3–27.3%.

Another important parameter that affects the still productivity is the temperature difference between water and glass cover which acts as a driving force of evaporation process. This effect can be enhanced by an external cooling of the glass cover [20–22]. Arunkumar et al. [23] carried out an experimental study in which water flow was used to cool the hemispherical still glass cover. They found that the productivity increases to about 15% and the efficiency was increased to 42%. Cooling the glass cover of a pyramid-shaped solar still using an external fan was investigated experimentally by Taamneh and Taamneh [24]. The results illustrates that the daily productivity was increased up to 25%.

Reducing the pressure inside the still is another way to increase the still productivity [25,26]. In their experimental study, Sriram et al. [27] used a vacuum pump to suck the vapor inside a single basin double slope solar still and to maintain vacuum pressure at 50 mmHg. Consequently, the still productivity was increased by 50.75%. In addition, integrating a separate condenser with the CSS increases the productivity by increasing the temperature difference between the water and the condenser wall and maintains the still at low pressure. It has been found that adding an external condenser increases the productivity by about 70–75% against the CSS [28–30]. Forced air convection inside the still was also used to increase the solar still productivity. This effect has not received enough attention where a few attempts have been addressed [4,31,32]. Ali et al. [33,34], studied the effect of air convection by placing a fan inside the CSS. He found that the still productivity is increased by about 30%. According to Lawrence and Tiwari [1], operation under natural circulation mode has been proven to be more advantageous in terms of simplicity, reliability and cost effectiveness. Fath et al. [28] found that about 75% of the still productivity is contributed through natural circulation with an efficiency increase of 50% in comparison to CSS.

In this work, an experimental attempt is made to improve the conventional single slope basin-type solar still thermal performances using an integrated Natural Circulation Loop (NCL). The air motion in this case is created by the buoyancy forces that evolve from the density gradients induced by the simultaneous effect of temperature and humidity between evaporator and condenser. The solar still was constructed and tested at the Faculty of Science and Applied Sciences, Oum-El-Bouaghi University, Algeria (Latitude: 35°79′N, Longitude 7°40′E). The tests were carried out in the period of June to July 2014 and the experimental data presented in this paper concerns four typical days. The constant C and n in the Nusselt relation were calculated from the experimental data and compared with those of Dunkle's model. The NC phenomenon inside the still has been investigated and the test data are compared with Vijayan's laminar model. The obtained experimental data show that the daily productivity of the proposed still is about 3.72 kg/m^2, the maximum hourly yield is 0.653 kg/m^2 h and the still efficiency can achieves 45.15%. Consequently, significant improvements are achieved in comparison with the CSS when air convection is created inside the still.

2. System design and experimentation

2.1. Solar still description

A schematic description of the proposed solar still is shown in Fig. 1. The still absorber was constructed with a rectangular galvanized plate of 0.35 m^2 (0.5 m × 0.7 m) with 1 mm of thickness and painted with black spray paint to increase the solar absorption. The absorber is encased in an airtight wooden box with a double glazing cover encloses the still surface. The still bottom side is insulated by glass wool of 10 cm thick to reduce the thermal losses. The still interior sidewalls are of 5 cm height and they are coated by white silicone for reflect solar radiation incident onto the saline water and acts as thermal barrier reducing heat losses [35]. The glass cover in the CSS has been replaced by a double glazing horizontal cover of 3 mm thickness for each glass. In fact, a horizontal cover coupled

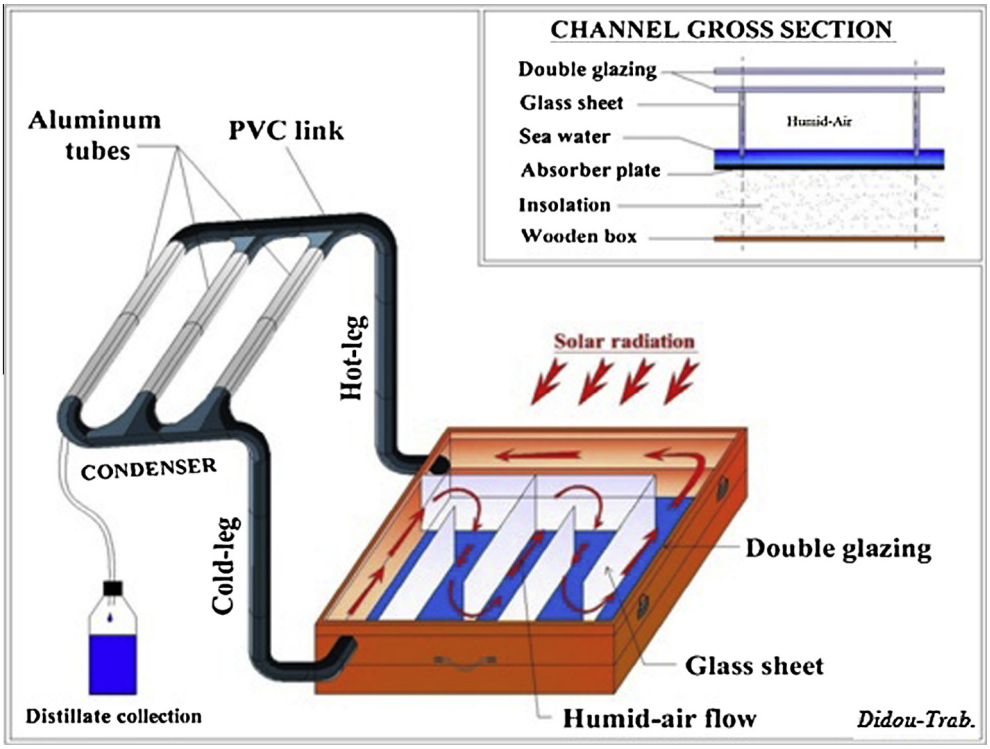

Fig. 1. Schematic illustration of the proposed solar still.

with an outside condenser could enhance the still efficiency up to 70–75% [29]. In addition, a gap of 15 mm between the glasses is estimated to minimize heat losses upwardly by about 25–35% [32]. Consequently, the condensation at the internal glass cover will be reduced and the generated moisture will be conveyed by air-flow then condensed in the cooler. The still air cavity is subdivided to several passes using vertical glass sheets which acting as baffles of 4.5 cm in height and separated between them by 10 cm. So, the fluid flow will be guided toward a long course in a rectangular duct. This partition allows forcing the air to pass through the evaporation surface, removing more moisture after leaving the evaporator and increase the fluid residence time in the heater. These baffles are suspended at the inner glass cover and submerged in the water to prevent air escape between the passes.

The condenser is a horizontal tubular heat exchanger in which the water steam is separated from the air and forms a condensate film. The heat exchanger is made of three parallel aluminum tubes of 700 mm length, 50 mm outer diameter and 1 mm of thickness for each tube. Aluminum is selected for its high conductivity and lightness. A slight inclination, of about 5°, to the condenser tubes is required to facilitate the drainage of the condensate water. The condenser is shaded from sun radiation by a plastic (sun-shade) cover placed above the condenser and spaced at 20 cm allowing the ambient air circulation around the condenser tubes. The link between the heater and the condenser is performed by two vertical PVC tubes of 80 mm diameter. These tubes were insulated by a glass wool layer of 2 cm of thickness and can be considered adiabatic. The distance between condenser and the heater is 0.5 m (from center to center). Two holes at the rear side of the still are provided to allow the vertical legs connections.

2.2. Working principle

The proposed solar still is designed to working as a Natural Circulation Loop (NCL) operating under the thermo-syphon effect with the humid-air as working fluid. Where the still serves as a heat source (heater), the condenser serves as a heat sink (cooler) and the vertical PVC tubes acting as hot and cold legs. Knowing that, NCL is one of the most effective ways that enables the fluid flow along a closed loop without a need for any external driving force [36]. Such systems are widely used for cooling purposes in industrial processes, including solar water heaters, geothermal processes, cooling electronic components, air conditioning, drying applications and as part of emergency core cooling system in nuclear power plants [37].

The solar radiation passes through glass cover is absorbed by the galvanized plate and then transferred to seawater contained in the basin within the still. The generated vapor is transferred to the flowing air which being heated and its density is decreased. In the condenser, the humid-air is being cooled and its density is increasing. The thermo-syphon effect acting to force the warm fluid to leave the heater and to go upwards through the hot-leg and directed to the condenser. After leaving the condenser, the cold dry air become heavy and returns toward the heater and repeat the process. So, a continuous circulation is takes place in the still enhancing both evaporation and condensation process and contributing to further increase in the still productivity. The water steam is separated from the air forming a thin liquid film which trickles down under the gravity effect and the little inclination of the condenser tubes. After that, the condensate film formed in the tubes trickles toward the water collection bottle.

2.3. Cost analysis

Economic analysis of the proposed still is performed according to Kabeel et al. [38] to estimate the still total annual cost base on the evaluation of fixed annual cost, the annual maintenance cost and the annual salvage cost. The annual fixed cost is obtained by multiplying the total fixed cost (P) by the amortization factor:

$$AFC = \frac{i(1+i)^n}{(1+i)^n - 1} P \quad (1)$$

where n, is the useful life of the still taken as 10 years and, i, is the rate of interest taken as 12% of the total fixed cost. The annual maintenance cost was considered as 10%. This cost covers the regular filling of water, collecting the distilled water, cleaning the glass cover and removal of salt deposited. The annual salvage cost is calculated by (Eq. (2)), where, S, is the salvage value taken as 20% of the total fixed cost.

$$ASC = \frac{i}{(1+i)^n - 1} S \quad (2)$$

Then, the system annual cost can be determined by:

$$AC = FAC + AMC - ASC \quad (3)$$

The average daily productivity of the still is assumed to be 2.5 kg/m^2. The unit is expected to operate 344 days in the year regarding to the sunshine duration characterizing the region of Oum El-Bouaghi-Algeria. Consequently, the cost of distilled water per liter is obtained by dividing the system annual cost by annual yield of the still. In fact, the main parts of the cost are for the labor costs which represent about 30% of the fabrication cost. The investment cost of each component constituting the proposed solar still is given in Table 1 and a summary of the cost evaluation analysis is presented in Table 2. Economic analysis shows that the cost of distilled water for the proposed still is 0.02 $/kg m^2 and the payback period of this system is 151 days.

3. Experimental setup

Fig. 2 shows a photograph of the experimental setup. The solar still was constructed and tested at the Faculty of Science and Applied Sciences, Oum-El-Bouaghi University, Algeria (Latitude: 35°79′N, Longitude 7°40′E). The tests were carried out in the period of June to July 2014 and the experimental data presented in this paper concerns four typical days. The still was filled with 3.5 kg seawater corresponding to 10 mm of water depth and oriented in north–south direction to receive solar radiation throughout the working hours of the day. During the experiment, the feed water is added at ambient temperature every half hour with an amount of water equal to that of distillate.

The experimental setup is suitably instrumented to measure the temperatures at different points in the still, relative humidity, total solar radiation and the amount of produced distillate. Calibrated K-type thermocouples are used to sense the wall temperature of the absorber, glass covers and the condenser external wall. Ambient temperature and basin water temperature are measured by digital thermometers WT-2 type. Humid-air temperature and relative humidity at the hot-leg and at the cold-leg are also measured using digital hygrometers. Solar radiation is measured by a CMP3-type pyranometer and wind velocity is measured using a Davis anemometer. A graduated transparent glass bottle of 1.5 L is used to collect and measure the condensate output. The K-type thermocouples and the pyranometer are connected to an automatic data acquisition system (VDAS) which displays the temperatures and the global radiation. All measured parameters are recorded every half-hour starting from 7:30 am to 6:00 pm. Table 3 shows the accuracies and error percentages of different measuring instruments used in the experiment. It has been found out that the maximum uncertainty in the measurements is about 3.1%.

Table 1
Cost estimation of the solar still components.

Unit components	Cost
PVC pipe and fittings	1100 DA ($ 13)
Glass cover	1300 DA ($ 15.4)
Galvanized plate	500 DA ($ 6.0)
Wooden box	1500 DA ($ 17.75)
Silicone paints and glues	700 DA ($ 8.3)
Insulation	600 DZ ($ 7.1)
Aluminum tube	600 DA ($ 7.1)
Labor cost	1900 DA ($ 22.5)
Total fixed cost	8200 DA ($ 97.1)
Total fixed cost per m^2	23,428 DA ($ 277)

1 USD = 84.5 DA.

Table 2
Economic analysis of the still.

Economic parameters and cost types	Value
Total fixed cost	97.1 $
Annual salvage cost	1.1 $ year^{-1}
Annual fixed cost	17.18 $ year^{-1}
Annual maintenance cost	1.72 $ year^{-1}
Annual water productivity	1032 kg/m^2
Cost of distilled water	0.26 $/kg
Total annual cost	17.8 $ year^{-1}
Cost of daily water produced	0.02 $/kg m^{-2}
Net profit	221.8 $ year^{-1}
Payback period	151 days

4. Results and analysis

4.1. Experimental data

The solar still thermal behavior during the four test days is described through the variations of its parameters given in Figs. 3–9. The solar radiation and ambient temperature variations are shown in Fig. 3. The ambient temperature was in the range of 23.2–41.5 °C and the solar radiation received during the study was in the range of 290–1015 W/m^2. Fig. 4 shows the variation of the wind speed measured each 30 min. for the four days. It is varied in the range of 0–5.8 m/s. The main temperatures describing the still behavior namely the absorber, brine water, glass covers, humid-air and the condenser wall temperatures for the test days are shown in Fig. 5. The humid-air temperature is evaluated by the arithmetic mean value calculated between hot-leg and cold-leg temperatures, $T_f = (T_H + T_C)/2$. It represents the fluid mean temperature through the loop knowing that both cold and hot legs are adiabatic. It is apparent that the meteorological conditions affect considerably the still thermal behavior. Variation of the accumulated an hourly yields during each test day is shown in Fig. 6.

4.2. Solar still thermal behavior

In order to analyze the still thermal behavior during a typical summer day, a simple approach is proposed. In which, the experimental data points are averaged over the four test days. It will therefore have a considerable degree of experimental uncertainty. Data of a particular measurement have been taken and an estimate of individual uncertainties of each data point has been calculated. The absolute error (ΔX) is estimated as the maximum error calculated between the experimental data point (X_i) and the mean value (X_m) by: $\Delta X = \max(X_m - X_i)$, where the real value has then been found as: $X = X_m \pm \Delta X$ [39]. Figs. 7–13 show the mean value of solar still thermal characteristics, where the corresponding maximum deviations are indicated by error bars.

Fig. 9 shows the temperature variation of absorber plate, brine water, glass covers, humid-air and the condenser wall for the standard metrological conditions during the test period. It is shown that, in the morning (08–10 h), the water temperature increases at a faster rate of about 13 °C/h, then it reaches its maximum of 68.6 °C at 13 h. The humid-air temperature in the heater increases

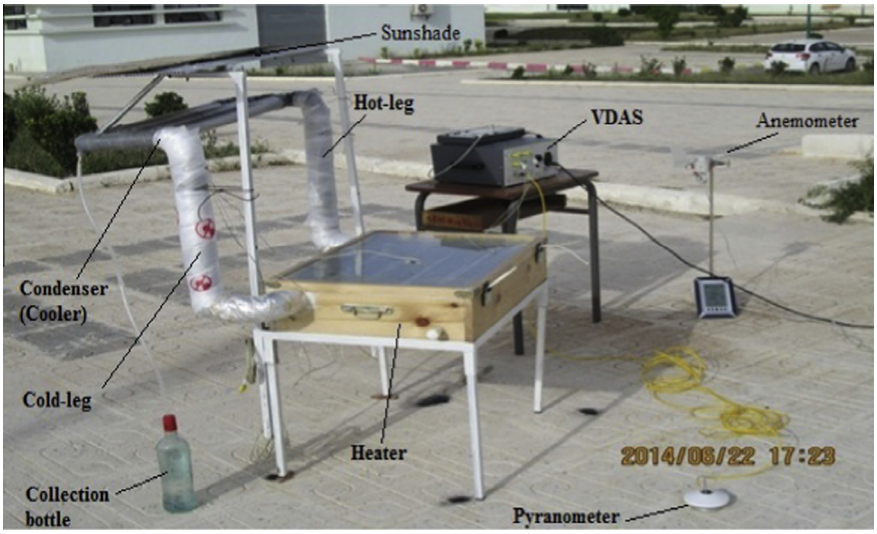

Fig. 2. A photograph of the experimental setup.

Table 3
Accuracies and error for measuring instruments.

Instrument	Accuracy	Range	% Error
K-type thermocouples	±1 °C	0–100 °C	1.4
Digital thermometers	±1 °C	−50–300 °C	1.5
Digital hygrometer	±5%	10–99%	7.1
Pyranometer	±1 W/m^2	0–2500 W/m^2	0.1
Davis anemometer	±0.1 m/s	0–50 m/s	2.0
Measure jar	±10 ml	0–1500 ml	0.6

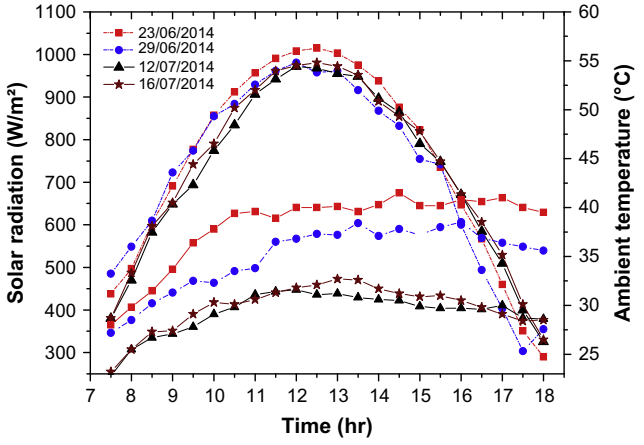

Fig. 3. Variations of solar radiation and ambient temperature on four different days.

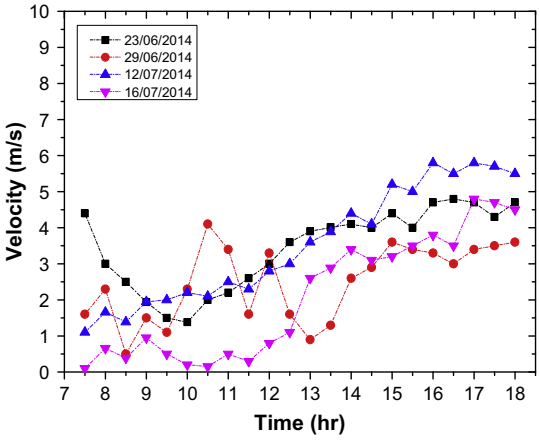

Fig. 4. Wind speed variation during the test days.

to about 57.86 °C and the internal glass cover temperature achieve 63.7 °C. The temperature difference between inner and outer glass covers is 21.57 °C. This confirms that the still cover design (zero inclination and double glazing), forms an effective thermal barrier to heat losses upwardly and contributing efficiently in increasing the water temperature at a faster rate. The maximum temperature difference between the water and the condenser wall is 25.45 °C. This difference is obtained from taking out the condenser from the still and from the high conductivity of the aluminum tubes forming the condenser. Between the water and the inner glass cover, the temperature difference (T_w–T_{gi}) is 5.5 °C. Where, it is 10.74 °C between the water and the humid-air in the heater (T_w–T_f). As a result, the heat and mass transfer is carried out from the water to the humid-air instead the inner glass cover. Fig. 10 shows the accumulated and hourly distillate produced as a function of daytime. The daily productivity achieved until 18 h is 3.72 l/m^2. The hourly yield of the still is characterized by a maximum of 0.653 l/m^2 h. Fig. 11 depicts the variation of the still efficiency with respect to time. The solar still efficiency (η) is calculated based on the mass of distilled water (m_d), the latent heat of evaporation (h_{fg}) and the total solar radiation (I_o) fall upon the still surface (A), according to Eq. (4) where the maximum still efficiency is approximately 45.15%.

$$\eta = \frac{m_d h_{fg}}{I_o A} \tag{4}$$

Figs. 12 and 13 show respectively the temperature and the relative humidity variations of the working fluid (humid-air) at the hot and cold legs. As the solar radiation is increased, the temperature difference would increase, consequently fluid relative humidity difference is enlarged. In the hot-leg, the working fluid is at high temperature and high relative humidity. whilst, in the cold-leg, both temperature and humidity are decreased. It can be concluded that the working fluid circulate in the desired direction under density difference between the heater and the cooler wherein it has been subjected to simultaneous heat and mass transfer.

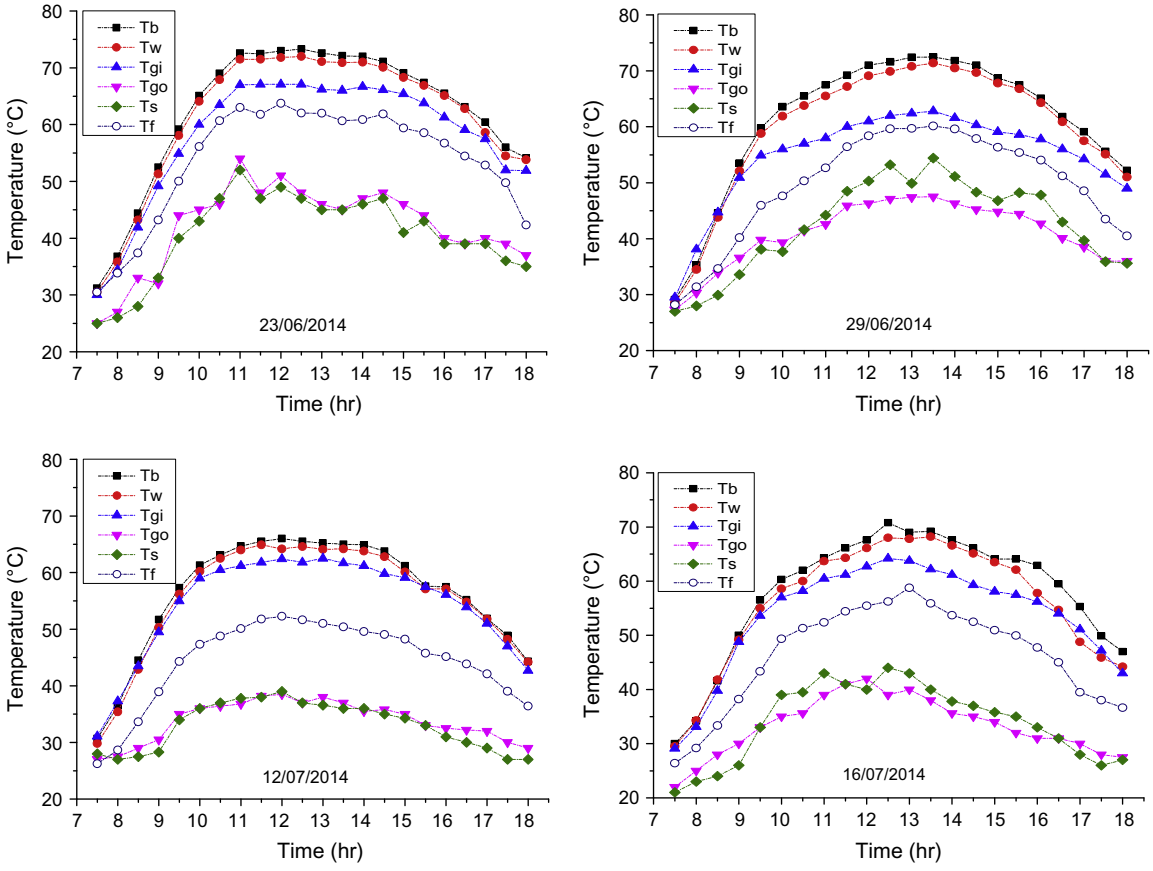

Fig. 5. Temperature variation at different locations in the still for the test days.

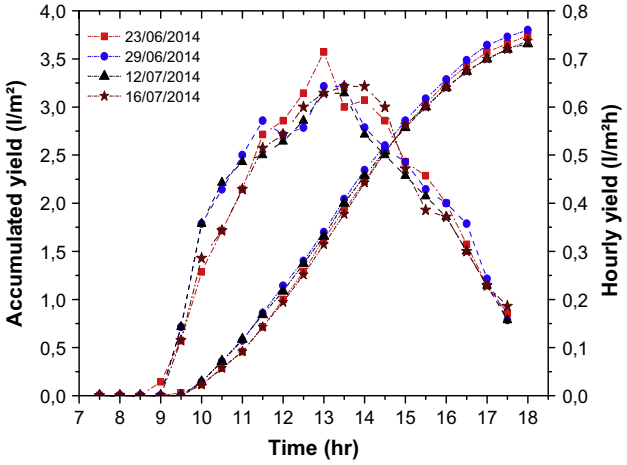

Fig. 6. Accumulated and hourly distillate production.

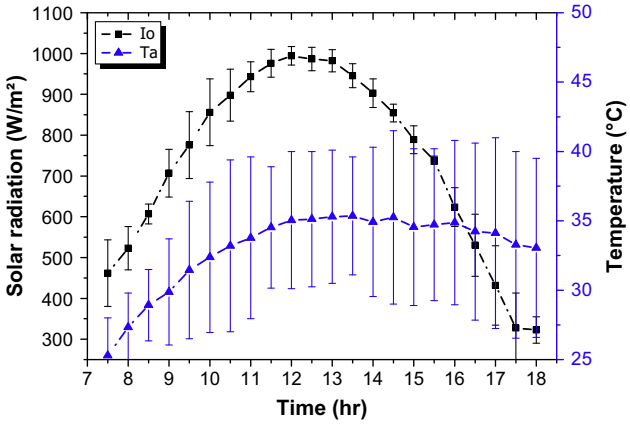

Fig. 7. Variations of solar radiation and ambient temperature.

4.3. Comparative analysis with previous studies

The comparative study between the obtained results and some previous experimental investigations [28,34,37] is presented in Table 4. These works have been carried out to study the effect of integrating passive condenser to the CSS under summer conditions. According to the system design, the water steam transfer from the still to the condenser can be either through purging-diffusion (due to pressure and vapor concentration difference) or by natural circulation (due to density difference between air inside still and condenser) [28]. It can be concluded that a large fraction of the resulting vapor condensed on the inner glass cover and the rest was transferred to the integrated external condenser. However, in our experiments, the entire produced vapor is transferred to the condenser.

5. Heat transfer analysis

The experimental data described by Figs. 7–13 are used to develop an empirical relationship describing the heat and mass transfer inside the proposed solar still. The internal heat transfer is considered between the water and the flowing humid-air. The heat transfer is carried out simultaneously by evaporation, convection and radiation where convection and evaporation are coupled

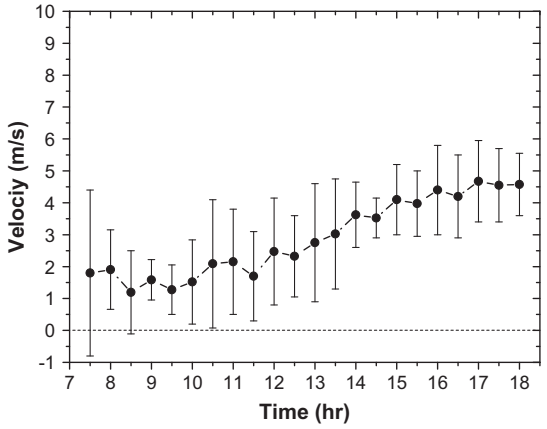

Fig. 8. Wind speed variation with time.

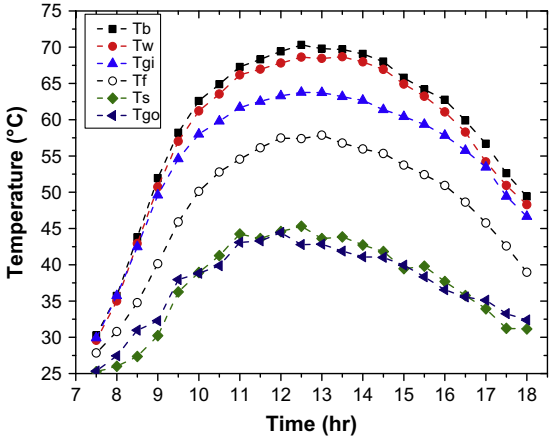

Fig. 9. Temperature variation at different locations in the still.

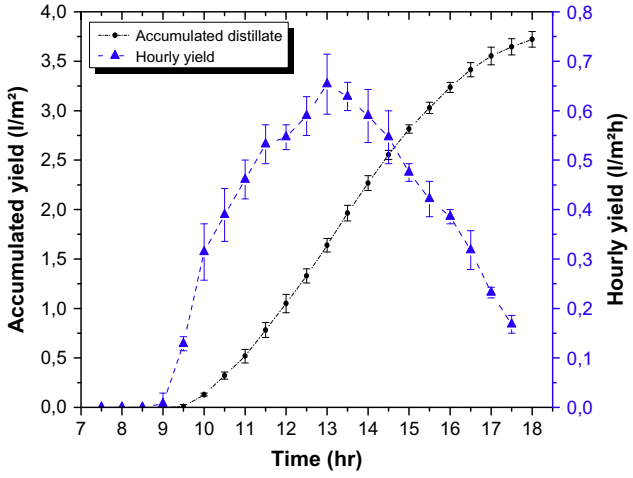

Fig. 10. Accumulated and hourly distillate production.

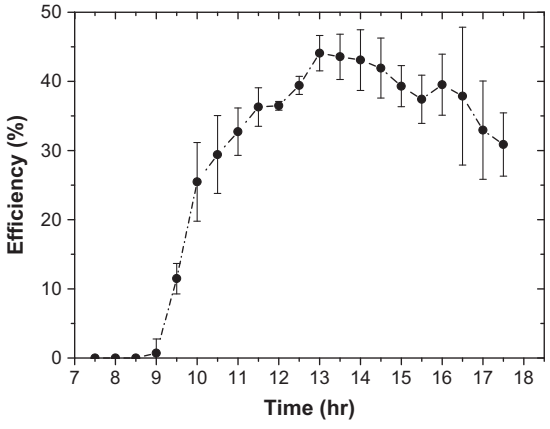

Fig. 11. Instantaneous variation of the solar still efficiency.

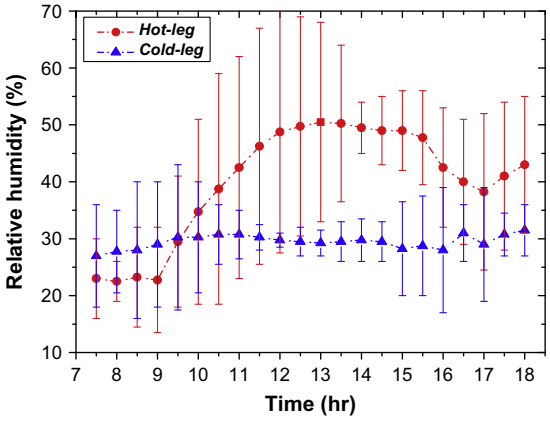

Fig. 12. Relative humidity variation at hot and cold-leg.

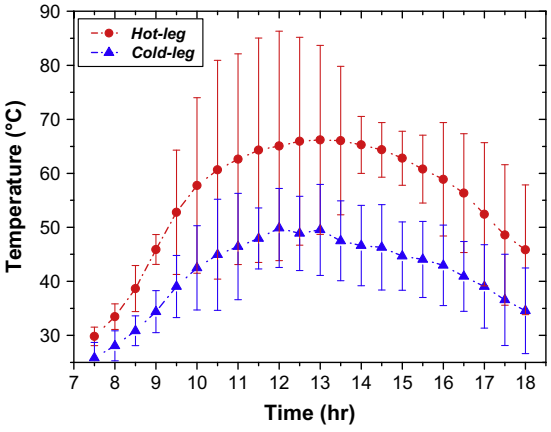

Fig. 13. Air temperature variation at the hot and cold-leg.

together. The experimental method used is a simple approach to evaluate the convective heat transfer coefficient based on the mass of the output distillate, the water temperature and both temperature and relative humidity of the working fluid. This empirical approach can be considered as a baseline support for thermal–hydraulic analysis and for future improvements in system design. The relationship of Nusselt number with the heat transfer coefficient h_{cw}, is given by the following expression [40]:

$$Nu = h_{cw}\frac{D}{k} = C(Gr' \cdot Pr)^n \tag{5}$$

where C and n are constants, P_r is the Prandtl number and Gr' is the modified Grashof number (Eq. (6)) for the simultaneous convective heat and mass transfer. Physical properties of humid-air as function of temperature are presented in Appendix A [11].

$$Pr = \frac{\mu C_p}{k}, \quad Gr' = \frac{\beta g D^3 \rho^2 \Delta T'}{\mu^2} \tag{6}$$

Table 4
Comparison with previous works.

No. Refs.	Working principle	Max. solar intensity (W/m^2)	Accumulated distillate (L/m^2 d)		Condenser contribution (%)
			From glass cover	From condenser	
Fath et al. [28]	Purging and diffusion	700	4.153	1.25	70
El-Bahi et al. [34]	Purging and diffusion	950	6.52	0.48	70
Husham et al. [37]	Purging and diffusion	1040	2.355	1.49	15.1
Husham et al. [37]	Natural circulation	1040	2.475	1.885	30.54
Present study	Natural circulation	1011	0.0	3.73	100

where

$$\Delta T' = (T_w - T_f) + \frac{(P_w - \varphi P_f)T_w}{268.9 \times 10^3 - p_w} \tag{7}$$

According to Dunkle [40], the convective heat transfer coefficient, h_{cw}, is given by:

$$h_{cw} = 0.884\Delta T'^{1/3} \tag{8}$$

where φ, is the mean relative humidity in the heater.

$$h_{ew} = 0.01623 h_{cw}\left[\frac{P_w - \varphi P_f}{T_w - T_f}\right] \tag{9}$$

By substituting Eq. (8) into Eq. (9), h_{ew} is obtained as follows:

$$h_{ew} = 0.01623\frac{k}{D}C(Gr'Pr)^n\left[\frac{P_w - \varphi P_f}{T_w - T_f}\right] \tag{10}$$

Further, the hourly yield per unit area can be calculated from:

$$m_d = \frac{h_{ew}(T_w - T_f)}{h_{fg}} \cdot 3600 \tag{11}$$

Substituting Eq. (10) into Eq. (11):

$$m_d = 0.01623(P_w - \varphi P_f)\left(\frac{k}{D}\right)\left(\frac{3600}{h_{fg}}\right)C(Gr'Pr)^n \tag{12}$$

Eq. (12) can be rewritten as:

$$\frac{m_d}{R} = C(Gr'Pr)^n \tag{13}$$

where $R = 0.01623(P_w - \varphi P_f)A_w\left(\frac{k}{D}\right)\left(\frac{3600}{h_{fg}}\right)$.

Eq. (13) can be reduced to a linear equation by taking logarithm on both sides:

$$ln\left[\frac{\dot{m}_{ew}}{R}\right] = lnC + nln(Gr'Pr) \tag{14}$$

Or, $y = lnC + nx$ (15)

where $\begin{cases} x = ln(Gr'Pr) \\ y = ln\left[\frac{\dot{m}_{ew}}{R}\right] \end{cases}$.

The unknown constants C and n (Eq. (5)) are determined by the linear regression analysis method presented in [11]:

$$n = \frac{\sum x \sum y - N\sum(xy)}{(\sum x)^2 - N\sum x^2} \tag{16}$$

$$C = exp\left(\frac{\sum y - n\sum x}{N}\right) \tag{17}$$

where N is the number of experimental observations. The experimental values of C and n obtained from the experimental data are 0.098 and 0.317 respectively. Then the dimensionless relationship of Nusselt number which characterizes the heat/mass transfer in the proposed still is given by:

$$Nu = 0.098(Gr'Pr)^{0.317} \tag{18}$$

Fig. 14 shows a comparison between the present model and Dunkle's model. Knowing that Dunkle's relation is applied for cavities that have parallel condensing and evaporative surfaces and the temperature range was about 25–60 °C. The constants value C and n in Dunkle's model are 0.075 and 1/3 respectively. Qualitatively, the convective heat transfer obtained by the present model (Eq. (18)) has the same asymptotic tendency like that of Dunkle's model. This implies that the heat transfer in the proposed still is temperature dependent. It is also observed that the convective heat transfer predicted by the present model exceed that given by Dunkle's model. This improvement is mainly due to the air convection created by the NC phenomenon which takes place in the still and contributes efficiently in its improvement.

It can be concluded that the NC heat and mass transfer capability is depends on buoyancy forces that evolve from the density gradients induced by the simultaneous effect of temperature and humidity. Compared with Dunkle's model, the deviation for the constants C and n in Eq. (18) is about 30.6% and 5%, respectively. The radiation heat transfer coefficient, h_{rw}, from water free surface toward the humid-air can be estimated by the following equation.

$$h_{rw} = \frac{\varepsilon_{eff} \cdot \sigma \cdot \left[T_w^2 + T_f^2\right] \cdot (T_w + T_f)}{\frac{1}{\varepsilon_f} + \frac{1}{\varepsilon_w} - 1} \tag{19}$$

The variation of convective, evaporative and radiative heat transfer coefficients with daytime is presented in Fig. 15. It is observed that the convective heat transfer coefficient is strongly temperature dependent (ie, proportional to the temperature difference between water surfaces and humid-air). While, the evaporative heat transfer coefficient have not the same tendency like the convective heat transfer coefficient this is due to its dependence on the partial vapor pressure which is very sensitive to temperature.

6. Natural circulation analysis

In this section, the natural circulation phenomenon inside the proposed solar still is studied based upon Vijayan's model assumptions [41]. The solar still is treated as a rectangular single-phase natural circulation loop with humid-air as working fluid. The total length of the loop is 4.55 m, the heated flow channel length is

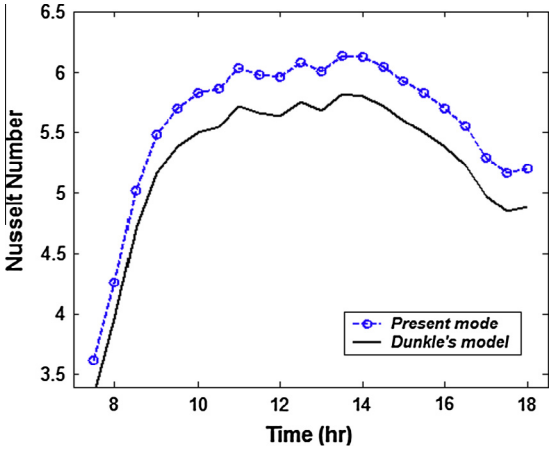

Fig. 14. Dunkle's model and experimental data.

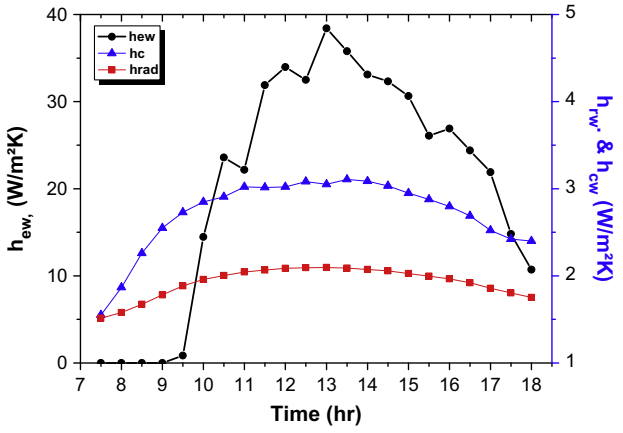

Fig. 15. Variations of evaporative, convective and radiative heat transfer coefficients.

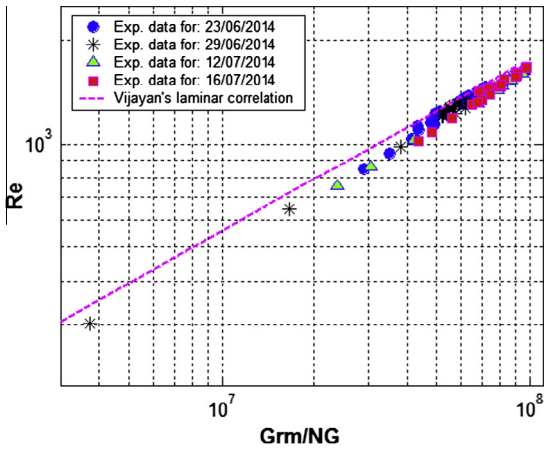

Fig. 16. Vijayan's laminar correlation and experimental data.

2.85 m and that of the condenser section is 0.7 m. The relative vertical distance between the center of the cooler and the heater (i.e. the driving head) is 0.5 m. with an aspect ratio of $L/D = 81$.

- One-dimensional steady-state fully developed flow approach is used.
- Temperature distribution in heating and cooling sections is linear.
- Vertical hot and cold legs are assumed adiabatic.
- The friction factor can be neglected and the bends effect can be considered by a proper friction coefficients.
- Effects of axial conduction are neglected and heat losses along the loop are negligible (<5%).
- Density variation may be assumed as linear function of temperature (Bossinesq approximation) as: $\rho = \rho_o[1 - \beta(T_f - T_o)]$. Where, ρ_o, is a reference density corresponding to the reference temperature T_o.

The governing momentum and energy equations describing the fluid flow behavior inside a closed loop are given by Eqs. (20) and (21) respectively. The integral momentum equation can be written as:

$$\frac{L}{A}\frac{dW}{dt} = g\rho_o\beta \oint Tdz - \frac{W^2}{2\rho_o A^2}\left(f\frac{L}{D} + k\right) \tag{20}$$

The energy equation varies along the loop can be expressed by:

$$\begin{cases} \frac{\partial T}{\partial t} + \frac{W}{\rho_o A}\frac{\partial T}{\partial s} = \frac{Q_H}{\rho_o CpAL}, & heater \\ \frac{\partial T}{\partial t} + \frac{W}{\rho_o A}\frac{\partial T}{\partial s} = -\frac{\pi D h_c (T - T_s)}{\rho_o CpA}, & cooler \\ \frac{\partial T}{\partial t} + \frac{W}{\rho_o A}\frac{\partial T}{\partial s} = 0, & legs \end{cases} \tag{21}$$

The loop behavior shows a quasi steady-state condition with a laminar fluid flow for the entire range of solar power input, since the system temperatures vary slowly. Therefore it is possible to drops all the time dependent terms. The steady-state solution for momentum and energy equations along the NC loop can be written according to the correlation presented by Vijayan [33]:

$$Re_{ss} = 0.1768\left[\frac{Gr_m}{N_G}\right]^{0.5} \tag{22}$$

$$Gr_m = \frac{g \cdot \beta \cdot D^3 \cdot \rho^2 \cdot Q \cdot H}{A \cdot Cp \cdot \mu^3} \tag{23}$$

where Gr_m is the modified Grashof number introduced by Vijayan [35,36,41], which depends on heat flux, geometry and fluid mean temperature. Q, is the heat transfer rate from the water to the working fluid obtained from the steady-state temperature rise across the heater as:

$$Q = WCp(T_H - T_C) \tag{24}$$

The steady-state flow rate in the natural circulation loop can be calculated by equating the driving buoyancy force with the resisting frictional force. Vijayan et al. [41] have derived the expression for the steady-state flow rate in a single-phase natural circulation loop as given by:

$$\dot{W} = \left[\frac{2\rho_o^2\beta g(T_H - T_C)H}{R}\right]^{\frac{1}{2}} \tag{25}$$

where H is the center line elevation difference between the cooler and the heater and R is the total hydraulic resistance of the loop given by:

$$R = \sum_{i=1}^{N}\left(\frac{fL}{D} + k\right)_i \frac{1}{A_i^2} \tag{26}$$

The parameter, N_G, is the contribution of loop geometry to the friction number [42,43] which is defined by:

$$N_G = \frac{L_t}{D_r}\sum_{i=1}^{N}\left(\frac{l_{eff}}{D^2 A}\right)_i \tag{27}$$

In the proposed loop is characterized by non-uniform loop diameters and cross sectional areas, then, reference diameter and reference areas are defined by:

$$D_r = \frac{1}{L_r}\sum_{i=1}^{N} D_i L_i, \quad A_r = \frac{1}{L_r}\sum_{i=1}^{N} A_i L_i = \frac{V_t}{L_t} \tag{28}$$

Comparative analysis (Fig. 16) shows that there is a good agreement between the Vijayan's laminar model (Eq. (22)) and the experimental data corresponding to the four test days. Knowing, that Vijayan's correlation was developed for large scale NC loops and it has been applied to the proposed solar still with humid-air as working fluid. Thus, it is clear that almost all data points are situated within the Reynolds numbers of 220–1670, near the transition regime. This confirm that heat and mass transfer enhancement (Fig. 15) is resulted from the use of the NC phenomenon which enables the fluid flow along the loop.

7. Conclusion

In the present work a new attempt is made to enhance the productivity of the conventional single slope basin-type solar still

using the thermo-syphon effect created by an integrated natural circulation loop. Some modifications are introduced to the CSS namely: building the solar still as a rectangular natural circulation loop, doubling the glass cover and using an external passive condenser, offers several advantages and contributes efficiently in the system improvement. From the results achieved in scope of this study, the following conclusions may be drawn:

- Separating the condenser from the still enlarges the temperature difference between the water and the condenser wall. So, a large difference in density can be obtained due to the difference in fluid thermodynamic conditions in each leg.
- The thermal–hydraulic characteristics related to the NC of humid-air in a closed loop can be reasonably captured by the present study. When, the NC capability in driving air convection in the still was demonstrated.
- Fluid flow in this case is created by the buoyancy forces that evolve from the density gradients induced by the simultaneous effect of temperature and humidity.
- Regression analysis method was used to develop the convective heat transfer relationship for the present solar still based on the experimental data. The comparison between the present correlation and Dunkle's model reveal that the heat transfer in the proposed solar still is temperature dependent. On the other hand, and due to the effects of the induced NC in the loop, the predicted model exceed the Dunkle's model.
- Using the relationship between Re_{ss} and Gr_m, the comparative analysis shows that there is a good trend between the experimental data and the Viajan's laminar correlation. In addition, the Reynolds number for the humid-air reaches high values of the order of 10^3.

Acknowledgements

The support provided by the University of Oum-El-Bouaghi, Algeria. Authors gratefully acknowledge Prof. Dib Abderrahmene, Dr. Mameri Abdelbaki, Dr. Mahfoudi El Ahcen Dr. Taïeb Oukssel and Dr. Djeddou Messaoud for their kind cooperation.

Appendix A

Physical properties of humid-air as function of temperature [11]:

$$T_i = \frac{T_H + T_C}{2}, \quad \varphi_i = \frac{\varphi_H + \varphi_C}{2}$$

$$\rho = \frac{353.44}{T_i + 273.15}, \quad \beta = \frac{1}{T_i + 273}$$

$$Cp = 999.2 + 0.1434T_i + 1.101 \cdot 10^{-4}T_i^2 - 6.7581 \cdot 10^{-8}T_i^3$$

$$k = 0.0244 + 0.7673 \cdot 10^{-4}T_i$$

$$\mu = 1.718 \cdot 10^{-5} + 4.62 \cdot 10^{-8}T_i$$

$$h_{fg} = 2.4935 \cdot 10^6[1 - 9.4779 \cdot 10^{-4}T_i + 1.3132 \cdot 10^{-7}T_i^2 - 4.7974 \cdot 10^{-9}T_i^3]$$

$$P_w = exp[25.317 - 5144/(T_w + 273)]$$

$$P_f = exp[25.317 - 5144/(T_f + 273)]$$

References

[1] Ayoub GM, Malaeb L. Developments in solar still desalination systems: a critical review. Environ Sci Tech 2012;42:2078–112.
[2] Omara ZM, Kabeel AE, Younes MM. Enhancing the stepped solar still performance using internal and external reflectors. Energy Convers Manage 2014;78:876–81.
[3] Hussain N, Rahim A. Utilization of new technique to improve the efficiency of horizontal solar desalination still. Desalination 2001;138:121–8.
[4] Dev R, Tiwari GN. Solar distillation. In: Ray C, Jain R, editors. Drinking water treatment-strategies for sustainability. Springer Science-Business, Media B.V; 2011. p. 159–210. http://dx.doi.org/10.1007/978-94-007-1104-4.
[5] He T, Yan L. Application of alternative energy integration technology in seawater desalination. Desalination 2009;249:104–8.
[6] Kabeel AE, Omara ZM, Essa FA. Enhancement of modified solar still integrated with external condenser using nanofluids: an experimental approach. Energy Convers Manage 2014;78:493–8.
[7] Ahsan A, Imteaz M, Thomas UA, Azmi M, Rahman A, Nik Daud NN. Parameters affecting the performance of a low cost solar still. Appl Energy 2014;114:924–30.
[8] Sivakumar V, Ganapathy SE. Improvement techniques of solar still efficiency: a review. Renew Sustain Energy Rev 2013;28:246–64.
[9] Omara ZM, Kabeel AE. The performance of different sand beds solar stills. Int J Green Energy 2014;11:240–54.
[10] Muftah AF, Alghoul MA, Fudholi A, Abdul-Majeed MM, Sopian K. Factors affecting basin type solar still productivity: a detailed review. Renew Sustain Energy Rev 2014;32:430–47.
[11] Tiwari AK, Tiwari GN. Effect of water depths on heat and mass transfer in a passive solar still in summer climatic condition. Desalination 2006;195:78–94.
[12] Tanaka H. Tilted wick solar still with flat plate bottom reflector. Desalination 2011;273:405–13.
[13] Tanaka H. Experimental study of a basin type solar still with internal and external reflectors in winter. Desalination 2009;249:130–4.
[14] Tanaka H, Nakatake Y. Theoretical analysis of a basin type solar still with internal and external reflectors. Desalination 2006;197:205–16.
[15] Abdallah S, Badran OO. Sun tracking system for productivity enhancement of solar still. Desalination 2008;220:669–76.
[16] Rajvanshi AK. Effect of various dyes on solar distillation. Sol Energy 1981;27:51–65.
[17] Badran OO. Experimental study of the enhancement parameters on a single slope solar still productivity. Desalination 2007;209:136–43.
[18] Velmurugan V, Gopalakrishnan M, Raghu R, Srithar K. Single basin solar still with fin for enhancing productivity. Energy Convers Manage 2008;49:2602–8.
[19] Abu-Hijleh B, Rababa HM. Experimental study of a solar still with sponge cubes in basin. Energy Convers Manage 2003;44:1411–8.
[20] Ahmed Z, Garni A. Enhancing the solar still using immersion type water heater productivity and the effect of external cooling fan in winter. Appl Sol Energy 2012;48:193–200.
[21] Suneesh PU, Jayaprakash R, Arunkumar T, Denkenberger D. Effect of air flow on "V" type solar still with cotton gauze cooling. Desalination 2014;337:1–5.
[22] Zurigat YH, AbuArabi MK. Modelling and performance analysis of a regenerative solar desalination unit. Appl Therm Eng 2004;24:1061–72.
[23] Arunkumar T, Jayaprakash R, Denkenberger D, Ahsan A, Okundamiya MS, et al. An experimental study on a hemispherical solar still. Desalination 2012;286:342–8.
[24] Taamneh Y, Taamneh MM. Performance of pyramid-shaped solar still: experimental study. Desalination 2012;291:65–8.
[25] Al-Kharabsheh S, Goswami Y. Experimental study of an innovative solar water desalination system utilizing a passive vacuum technique. Sol Energy 2003;75:395–402.
[26] Kabeel AE, Omara ZM, Essa FA. Improving the performance of solar still by using nanofluids and providing vacuum. Energy Convers Manage 2014;86:268–74.
[27] Sriram V, Samuel Hansen R, Kalidasa Murugavel K. Experimental study on a low pressure solar still. Appl Sol Energy 2013;49:137–41.
[28] Fath HES, Elsherbiny SM. Effect of adding a passive condenser on solar still performance. Energy Convers Manage 1993;34:63–72.
[29] Smolsky BM, Sergegev GT. Heat and mass transfer with liquid evaporation. Heat Mass Transf 1962;5:1011–21.
[30] Malik MAS, Tiware GN, Kumar A, Sodha MS. Solar distillation. Oxford, UK: Pergamon Press; 1982.
[31] Ali HM. Experimental study on air motion effect inside the solar still on still performance. Energy Convers Manage 1991;32:67–70.
[32] Ali HM. Effect of forced convection inside the solar still on heat and mass transfer coefficients. Energy Convers Manage 1993;34:73–9.
[33] Tenthani C, Madhlopa A, Kimambo CZ. Improved solar still for water purification. J Sustain Energy Environ 2012;3:111–3.
[34] El-Bahi A, Inan D. A solar still with minimum inclination, coupled to an outside condenser. Desalination 1999;123:79–83.
[35] Kumar KK, Gopal MR. Experimental studies on CO_2 based single and two-phase natural circulation loops. Appl Therm Eng 2011;31:3437–43.
[36] Nayak AK, Gartia MR, Vijayan PK. An experimental investigation of single-phase natural circulation behavior in a rectangular loop with Al_2O_3 nanofluids. Exp Therm Fluid Sci 2008;33:184–9.
[37] Husham MA. Seasonal performance evaluation of solar stills connected to passive external condensers. Sci Res Essays 2012;7:1444–60.
[38] Kabeel AE, Hamed AM, El-Agouz SA. Cost analysis of different 20 solar still configurations. Energy 2010;35:2901–8.
[39] Kline SJ, McClintock FA. Describing uncertainties in single sample experiments. Mech Eng 1953;75:3–8.

[40] Kumar S, Tiwari GN. Estimation of convective mass transfer in solar distillation system. Sol Energy 1996;57:459–64.
[41] Tiwari GN, Shukla SK, Singh IP. Computer modeling of passive/active solar stills by using inner glass temperature. Desalination 2003;154:171–85.
[42] Misale M, Garibaldi P, Passos JC, Ghisi de Bitencourt G. Experiments in a single-phase natural circulation mini-loop. Exp Ther Fluid Sci 2007;31:1111–20.
[43] Vijayan PK. Experimental observations on the general trends of the steady state and stability behavior of single-phase natural circulation loops. Nucl Eng Des 2002;215:139–52.